Hemoglobin Bioconjugates with Surface-Protected Gold Nanoparticles in Aqueous Media: The Stability Depends on Solution pH and Protein Properties.

*Rafael del Caño,[1] Lucia Mateus,[1,2] Guadalupe Sánchez-Obrero,[1] José Manuel Sevilla,[1] Rafael Madueño,[1] Manuel Blázquez,[1] Teresa Pineda[1]**

[1] Department of Physical Chemistry and Applied Thermodynamics. Institute of Fine Chemistry and Nanochemistry. University of Cordoba, Campus Rabanales, Ed. Marie Curie 2ª Planta, E-14014 Córdoba, Spain

[2] Present address: Corporación Tecnológica de Bogotá, Bogotá, Colombia.

AUTHOR EMAIL ADDRESS tpineda@uco.es

AUTHOR ORCID Nº: 0000-0002-1504-903X

Phone number: +34-957-218646

Fax number: +34-957-218618

Abstract

The identification of the factors that dictate the formation and physicochemical properties of protein-nanomaterial bioconjugates are important to understand their behavior in biological systems. The present work deals with the formation and characterization of bioconjugates made of the protein hemoglobin (Hb) and gold nanoparticles (AuNP) capped with three different molecular layers (citrate anions (c), 6-mercaptopurine (MP) and ω-mercaptoundecanoic acid (MUA)). The main focus is on the behavior of the bioconjugates in aqueous buffered solutions in a wide pH range. The stability of the bioconjugates have been studied by UV-visible spectroscopy by following the changes in the localized surface resonance plasmon band (LSRP), Dynamic light scattering (DLS) and zeta-potential pH titrations. It has been found that they are stable in neutral and alkaline solutions and, at pH lower than the protein isoelectric point, aggregation takes place. Although the surface chemical properties of the AuNPs confer different properties in respect to colloidal stability, once the bioconjugates are formed their properties are dictated by the Hb protein *corona*. The protein secondary structure, as analyzed by Attenuated total reflectance infrared (ATR-IR) spectroscopy, seems to be maintained under the conditions of colloidal stability but some small changes in protein conformation take place when the bioconjugates aggregate. These findings highlight the importance to keep the protein structure upon interaction with nanomaterials to drive the stability of the bioconjugates.

Keywords: hemoglobin, gold nanoparticles, protein *corona*, UV-visible spectroscopy, attenuated total reflectance infrared spectroscopy, dynamic light scattering, zeta-potential,

1. Introduction

The interaction of nanomaterials (NMs) with the biological environment is mainly studied to understand their *in vivo* behavior and to help in the rational design of drug delivery systems, being the interaction of NMs with biomolecules of fundamental interest [1]. It is accepted that protein adsorption takes place as soon as the NMs contact the biological milieu producing changes in the biological identity of the NMs as the surface is surrounded by a *corona* of proteins. This protein *corona* acts as the primary antenna and interacts with the biological machinery for further cellular interactions [2-4]. The concept of protein *corona* that was first defined by Dawson and coworkers [5-7] states that when the NMs are dispersed in a biological system, they are readily covered by a dynamic coating of biomolecules, mainly proteins. The protein *corona* is not spatially homogeneous. The inner layer (hard *corona*) exchanges slowly with the proteins in solution but the external layers (soft *corona*) are composed of weakly bound proteins that

exchange very fast [8]. Recently, however, a new concept brings about the idea that the protein *corona* is more complex than it was thought and it is established rapidly, and their formation more likely occurs to varying degrees for all kind of NMs [9].

In the context of NMs, plasma and serum are the most widely studied biological systems because blood is the primary travelling fluid when NMs are applying to living organisms. One important point is that the biological signals of the surface-adsorbed proteins remains elusive with regard to whether the conformation of the adsorbed proteins is different from that of its native state [10]. The three-dimensional conformation of the different proteins on NMs are presumably different from their native states, but how this uncharacterized discrepancy for either a single protein or a combination of protein libraries affect the NM-cell and NM-body interactions remain to be explored [1, 2, 11, 12]. In fact, the lack of knowledge of the interactions between NMs and the physiological environment such as blood and interstitial fluids is one of the main reasons why the clinical setting of these systems is not yet established [13]. The biological fluids are composed of electrolytes, proteins, lipids, and metabolites, and all these components can adsorb onto the surface of the NMs [4, 14-18]. The new layers that surround the NM shields the original surface properties and alter the size and composition providing the NPs with a new biological identity [3, 17, 19].

The widespread applicability of gold nanoparticles (AuNPs) is due to the unique size-dependent chemical, physical and optical properties they exhibit, along with the ease in which they can be functionalized by biological relevant chemistries [20]. The precise design of AuNPs for the efficient incorporation in biological milieu is necessary to understand how these materials and their properties are altered and, how the components of the biological milieu respond to their presence. Therefore, the fundamental physicochemical description of the gold-bio interface should be known. This knowledge includes the conformation of the proteins that form the hard and, when possible, the soft *corona*. Moreover, the development of new strategies to create NPs with predictable/controllable biological identity by coating with specific proteins is a promising way to control *corona* formation, mainly via protein-protein interactions, and enhanced targeting by recruiting proteins from biological milieu. In this sense, the optimization of nanoparticle surface properties by either protein-pre-coating or specific chemical modifications can gain in accessibility of their active sites to the cell receptors.

In general, because of the size and route of administration, NPs can easily reach the bloodstream and the first biological entity they encounter are red blood cells (RBCs). Zhao et al [21] have found that silica NPs of different sizes and surface properties interact with human RBCs yielding toxicity, first for the binding of the silanol-rich surface of the NPs to the phosphatidylcholine molecules present on the cell membrane, and then by producing the bending of the membrane to adapt to the rigid surface of silica, which caused cell disruption. Although the formation of the protein *corona* on the NPs upon contact with the blood fluids mitigate or suppress hemolysis, there is no information of how much protein is necessary

or how intrinsic proteins as Hb contribute to this phenomenon. In this sense, an elegant study of SERS spectroscopy on the interaction of gold and silver nanoparticles with RBCs [22] indicates the interaction of nanoparticles with these cells as well as the Hb proteins and other red blood cell components. The authors conclude that the use of this spectral information will help to learn more about the role of the erythrocyte membrane in nanoparticle uptake.

Thus, it is of great interest to study the interaction of Hb with different NPs and this protein has been chosen in the present study as a case for the characterization of protein-AuNP biochemical complex. There have been previous attempts to study the bioconjugates formed with Hb and gold or silver nanoparticles [22-28] but any of them have addressed the behavior in aqueous solutions under different pH conditions to examine the stability against aggregation. In the present work, we carried out the study of the bioconjugates formed upon mixing Hb with AuNPs protected by citrate anions (c), 6-mercaptopurine (MP) and ω-mercaptoundecanoic acid (MUA). The characterization of the bioconjugates is performed by using spectroscopic techniques such as UV-visible and ATR-IR, dynamic light scattering and zeta-potential measurements. We are interested in the evaluation of the stability of the bioconjugates formed with surface-protected AuNPs with different chemical identity, the possible conformational changes in the protein structure upon interaction with the nanoparticles and how these features are influenced by the solution pH.

2. Experimental Section

2.1.Reactants.

Hb, from bovine blood, MP, MUA, Hydrogen tetrachloroaurate trihydrate and semiconductor grade purity sodium hydroxide were purchased from Sigma-Aldrich. The rest of the reactants were from Merck analytical grade. All solutions were prepared with deionized water produced by Millipore system.

2.2.Synthesis of cAuNPs.

The synthesis of cAuNPs (15 nm diameter, Figure SI-1) has been carried out by following a classic method [29] consisting of the reduction of $HAuCl_4$ by citrate anions in an aqueous medium. The synthesis of MP-AuNPs and MUA-AuNPs has been carried out by adding a 10-fold excess of either MP or MUA to a cAuNPs alkaline aqueous solution. The samples of MP- and MUA-AuNPs were dialyzed against a 10 mM NaOH solution to remove the excess of reactant. The formation of the self-assembled monolayer concomitant to the displacement of citrate ions from the AuNP surface has been demonstrated by FT-IR spectroscopy [30, 31].

2.3.Formation of the Bioconjugates.

To avoid aggregation, the bioconjugates have been formed by mixing the appropriate amounts of AuNPs and protein in aqueous solution at pH 12 and incubating at a temperature of 4 ºC for at least 30

min. The stock solutions of the bioconjugates are then used for the different experiments by diluting in the buffer of interest or centrifuging to get more concentrated preparations. The studies of the influence of pH have been carried out by titration experiments starting at pH 12.

2.4.Characterization Techniques.

The absorbance spectra were recorded using a Jasco V-670 UV−vis−NIR spectrophotometer. ATR infrared spectra were recorded on a JASCO 6300 FTIR single (He-Ne) laser beam spectrometer in the 1000-4000 cm^{-1} wavenumbers range, and the data were acquired by the integrated software (Spectra Manager). A variable angle specular reflectance accessory (Pike Technologies-VeeMAX^{TM}) assembled in the FTIR spectrometer compartment enabled samples to be analyzed at different beam incident angles. A germanium crystal with an orientation of 60 º was used. The spectra were collected using an uncooled single element DTGS–detector. Then, a total of 256 spectral scans were averaged at a spectral resolution of 2 cm^{-1} in the frequency window of 4000 to 1000 cm^{-1}. First, after baseline corrected, the spectra were selected in the amide I region (i.e., 1600-1700 cm^{-1}). Then, the spectra were processed calculating second derivatives, and the obtained peaks frequencies as well as accepted literature data were used to fit using Gaussians functions [32-34]. A multiple peak fitting technique using Micro Cal Origin 7.0 was employed, that includes the width, area and frequency position of all bands as fitting parameters. This multicomponent fitting allows us to identify different components and the corresponding peak frequencies. The percentage area of the deconvoluted peaks gives the relative amounts of the components. Prior to the measurements, the interferometer and the sample compartments were purged with a dry and free CO_2 air flux of 8 L/min, supplied by a compressed air adsorption dryer (K-MT LAB, Parker/Zandet GmbH&Co.KG).

Dynamic light scattering (DLS) and Zeta-potential analysis were performed to evaluate the hydrodynamic diameter and surface charge of AuNPs in the absence and presence of Hb at room temperature using Malvern Zetasizer Nano, ZSP with 633 nm He−Ne laser, equipped with a MPT-2 Autotitrator. The measured data are the average of at least 20 runs. The average hydrodynamic diameter and mean zeta potential of each sample were computed using the software provided by the manufacturer.

3. Results and Discussion

3.1.UV-visible spectroscopy.

The modification of the surface of cAuNPs through SAM by using mercapto-derivatives such as MP and MUA brings about changes in the LSPR band position of several nanometers (Figure SI-2) due to the change in the dielectric constant of the media surrounding the AuNPs [35]. When the molecular layer formed around the AuNP is thicker, as it is the case for the protein *corona* formed in the biological media, the displacement is also observed but it is not larger than that obtained in the presence of the SAM. In

fact, the changes observed when the protein Hb is added to the AuNPs solution is of around 6 nm, as it has been observed with other proteins [36, 37]. Figure 1 shows the spectra obtained for a solution of cAuNPs in the presence of increasing concentrations of Hb. When the Hb/cAuNP molar ratio is 200/1, the LSPR band reach a shape that is kept constant upon further protein additions. The small displacement observed in the LSPR band is taken as a first proof that the protein *corona* has been formed [36, 37]. The signal observed at 406 nm corresponds to the Soret band of Hb that is typical for the met-Hb that is the stable species in 10 mM phosphate buffer at pH 7.4.

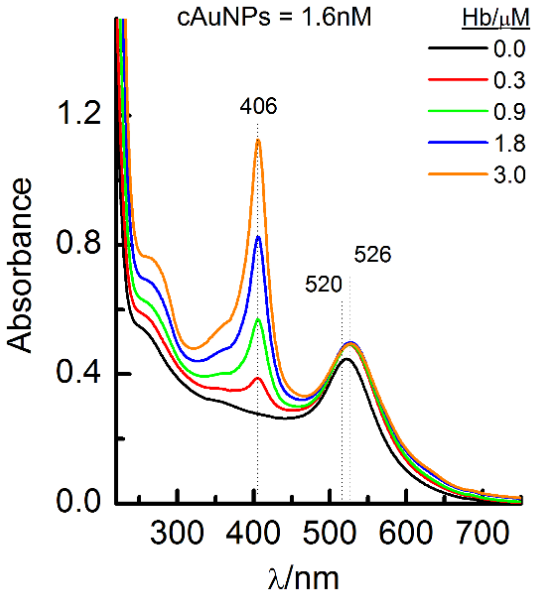

Figure 1. UV-visible spectra of Hb-cAuNPs at different Hb/cAuNPs molar ratios, in phosphate buffer 10 mM at pH 7.4.

We use the molar ratio of 200/1 in further experiments to warrant that the protein *corona* is formed and to avoid the influence of bigger amounts of free protein in the spectra. We have observed a similar LSPR band displacement when the bioconjugates are formed by MP- and MUA-AuNPs, and the saturation molar ratios are also reached at values close to 200/1.

To get more insight into the nature of the bioconjugates formed, the influence of the medium pH has been analyzed for the three bioconjugates. In Figure 2, the displacements of the LSPR bands in the absence and presence of protein are plotted.

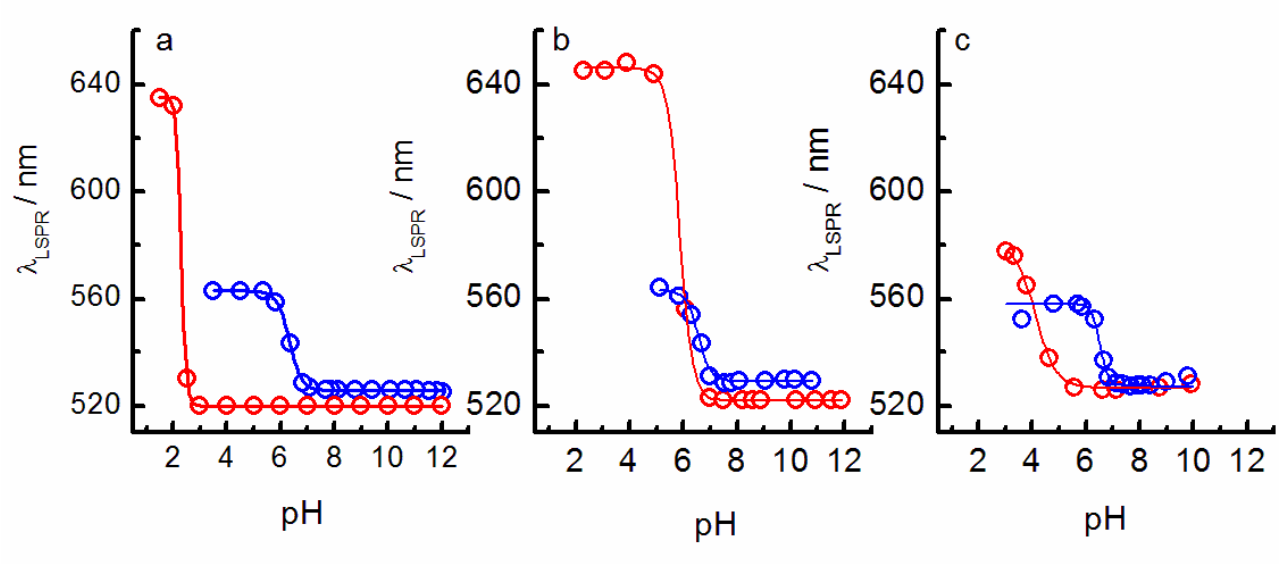

Figure 2. Changes in the LSPR wavelength as a function of solution pH. (a) cAuNPs; (b) MP-AuNPs; (c) MUA-AuNPs; Red: AuNPs; Blue: Hb-AuNPs. The pH titration has been made at a molar ratio Hb/AuNP of 200/1, in 10 mM phosphate buffer.

The AuNPs either stabilized by citrate anions or mercapto-derivative molecules behave very differently in respect to the LSPR wavelength band displacement and the inflection point for flocculation. It can be said that they obey to the chemistry of the protected layer [37]. However, the corresponding bioconjugates show a very similar pattern. In fact, LSPR shifts of 38, 32 and 34 nm and inflection points of 6.3, 6.5 and 6.5 for the bioconjugates formed with c-, MP- and MUA-AuNPs, respectively, are found. These features are indicative of the formation of a Hb *corona* on the AuNP surface which global structure is independent on the nanoparticle surface modification and the aggregation phenomena only takes place after changing the global charge of the bioconjugate.

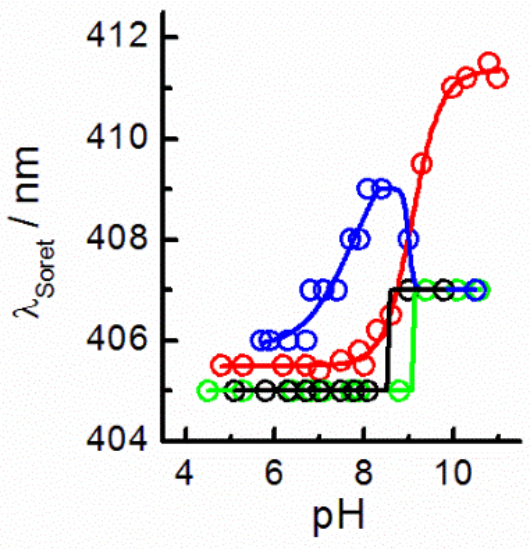

Figure 3. Changes in the Soret wavelength band of: Red: free Hb; Black: Hb-cAuNPs; Green: Hb-MP-AuNPs. Blue: Hb-MUA-AuNPs. The pH titration has been made at a molar ratio Hb/AuNP of 200/1, in 10 mM phosphate buffer.

Some aspects related to the Hb conformation are worthwhile to consider in these experiments. One of the most characteristic features of the Hb protein is the position of the Soret band that, for met-Hb is of 405 nm. In this species, the heme iron is in a six-coordinated high spin complex, being the sixth position occupied by a H_2O molecule. As it can be seen in Figure 3, the Soret band is kept at 405 nm from mild acid to basic conditions, where a change to 411 nm is observed with an inflection at pH ~ 9. This change is produced by the dissociation of the H_2O molecule to OH^- [38]. We have measured the changes in the Soret band of Hb bound to the AuNPs and only in the case of the bioconjugate formed by MUA-AuNPs, the Soret band increases at neutral pH describing an inflection at 7.7, more than one pH unit lower than the free protein. However, upon the dissociation of the heme coordinated water molecule, the wavelength decreases and reaches the value of 407 nm. In the case of the Hb-cAuNP and Hb-MP-AuNP, the change in the Soret band takes place at a pH value close to the free protein although the final value is lower and coincides with this of the Hb-MUA-AuNP bioconjugates. As these changes are only related to the structure of the heme region, they could indicate that the orientation of the proteins in the *corona* external layer protects the heme environment against the changes with the solution pH. In this sense, the different behavior observed for the Hb-MUA-AuNPs bioconjugates could be explained by a different orientation of the protein probably due to the higher negative charge density on the MUA-AuNPs in comparison to c- and MP-AuNPs surfaces in the middle pH range.

3.2.Dynamic light scattering (DLS) and zeta-potential measurements.

DLS technique can be readily used as a tool to reveal the formation of the Hb-AuNP bioconjugates and to detect the existence of any aggregation phenomena. Thus, a pH titration experiment has been carried out by recording the hydrodynamic diameter (D_H). As it is observed in Figure 4, the size of the cAuNPs is kept constant from alkaline to weakly acid medium. At pH lower than 5, the size suddenly increases indicating the formation of big aggregates. If the dissociation pK of the citrate anions are taken in mind, the reduction in negative charge produced upon lowering the solution pH, can provoke either the decrease of repulsion forces or the desorption of citrate anions from the AuNP surfaces [39]. The bioconjugates follow a similar trend, with a larger D_H value than this of the cAuNPs, indicating protein *corona* formation. However, aggregation takes place suddenly at pH 6. This is in agreement with the UV-Visible results that show the displacement of the LSPR band at higher wavelengths in this pH interval. In a first step, higher sizes of aggregates are measured but, after decreasing pH, the size start to decrease describing

a decay curve that becomes stationary at acid pH. This effect that is also observed with the cAuNPs although in a lower extension is, in fact, only an apparent result. A comparison to the UV-visible spectra of the bioconjugates in this pH range makes clear that the absorbance of the LSPR band at pH 3 decreases in respect to these recorded at pH 5 and 8. The explanation of this effect can be that the bigger aggregates formed precipitate, and the spectrum at pH 3 as well as the diameter measured by DLS only correspond to the aggregates that remain in solution that are these of lower size.

From these results, we can conclude that the bioconjugates are formed and are stable in alkaline and neutral solutions. At lower pHs they aggregate, continuing in solution only those of smaller sizes.

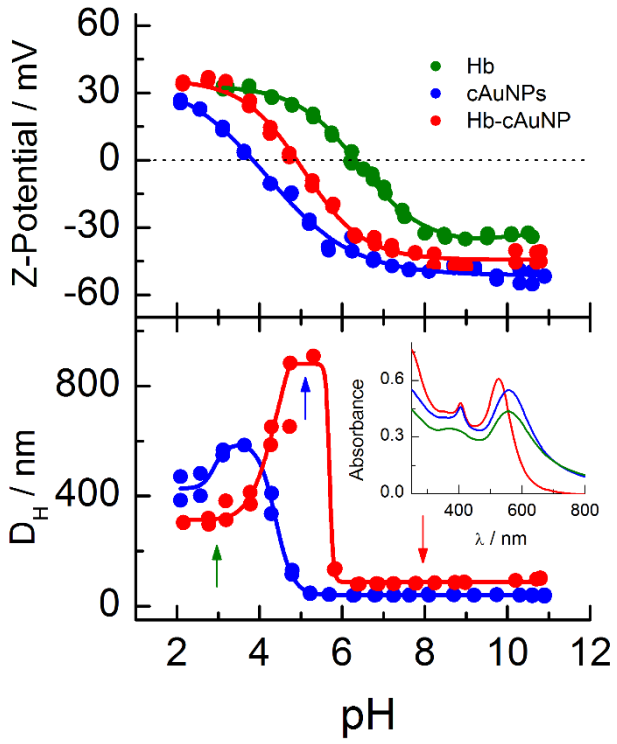

Figure 4. DLS (lower panel) and zeta potentials (higher panel) obtained in the titration of cAuNPs, Hb and Hb-cAuNPs as a function of pH. Insert: UV-visible spectra of the bioconjugates at different pHs under the same experimental conditions. The colored arrows in the titration curves correspond to the different pH of the spectra.

We have also measured Zeta-potential of these samples. Starting with the free protein, a negative value of -34 mV is obtained in alkaline aqueous solution that slowly changes to positive values (+32 mV) with an isoelectric point (IP) of 6.3 in agreement with literature data for the Hb protein. The cAuNPs also show a negative value of -50 mV in alkaline media where the capping citrate anions are completely dissociated. This value is maintained up to pH values where the citrate anions are neutralized (IP 3.8). Finally, the bioconjugates Hb-cAuNPs show an intermediate behavior changing from -44 mV in alkaline to +35 mV

in acid media. The IP obtained for the bioconjugates is 4.9, more than one pH unit lower than that of the free protein, indicating that the positive charges of the protein are somewhat neutralized or hidden upon protein *corona* formation.

It is interesting to note that the bioconjugates start to aggregate upon the Zeta-potential increases and that the aggregates formed are one order of magnitude larger than the isolated bioconjugates that are stable at neutral and alkaline pH (Scheme 1).

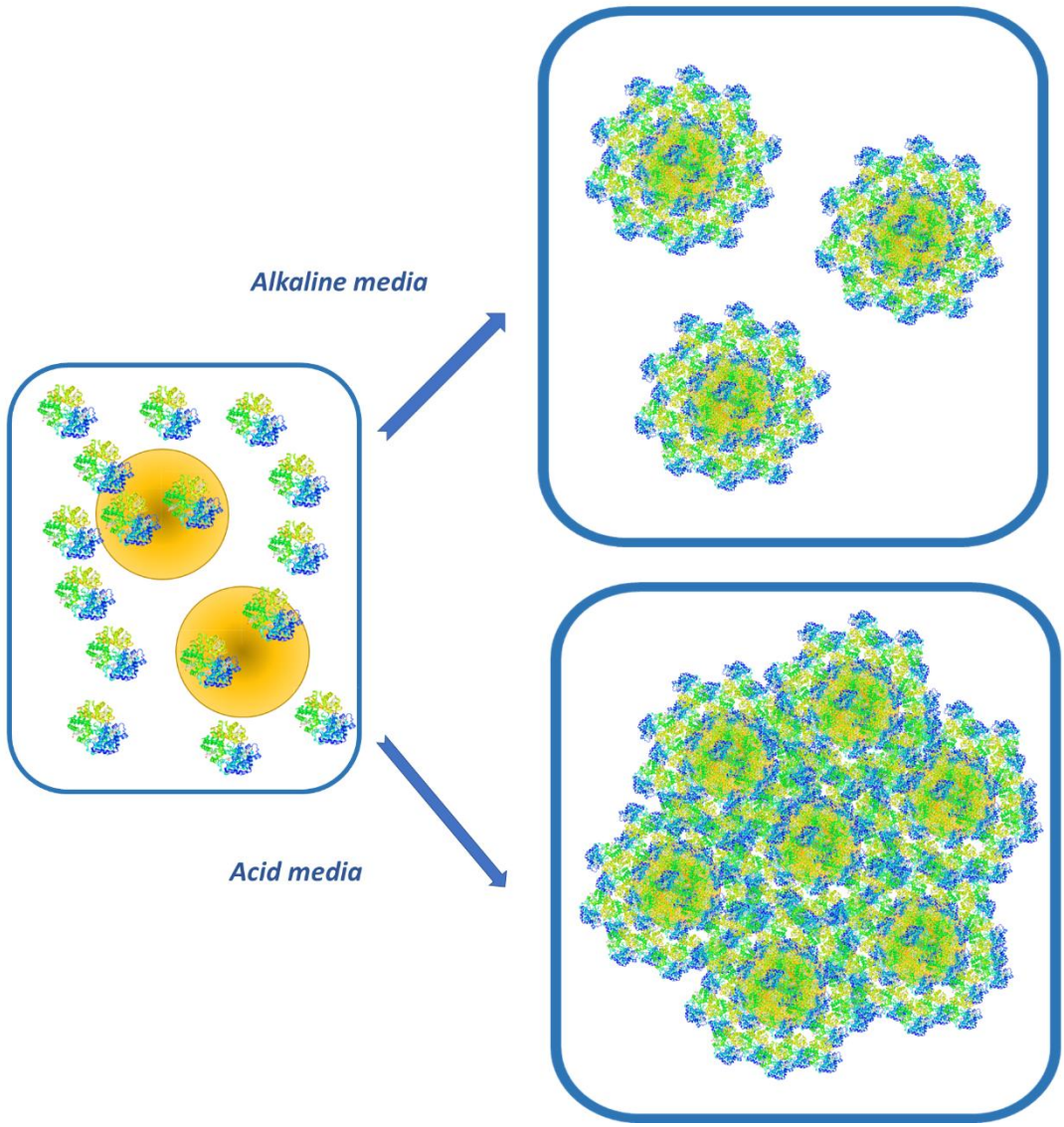

Scheme 1

3.3.Infrared characterization.

IR spectroscopy is a highly sensitive tool for examining proteins secondary structure and this is probed by the study of the characteristic amide I and amide II bands. Whereas the amide I band (1600-1700 cm^{-1}) is attributed to the C=O stretching vibrations of peptide linkages in the protein backbone, the amide II

(1500-1600 cm^{-1}) results form a combination of N-H bending and C-N stretching vibrations. The amide I is sensitive to the peptide secondary structure like α-helices, β-sheets and β-turns as the corresponding band energies depend on the hydrogen bond strength between the amide units [32, 33, 40].

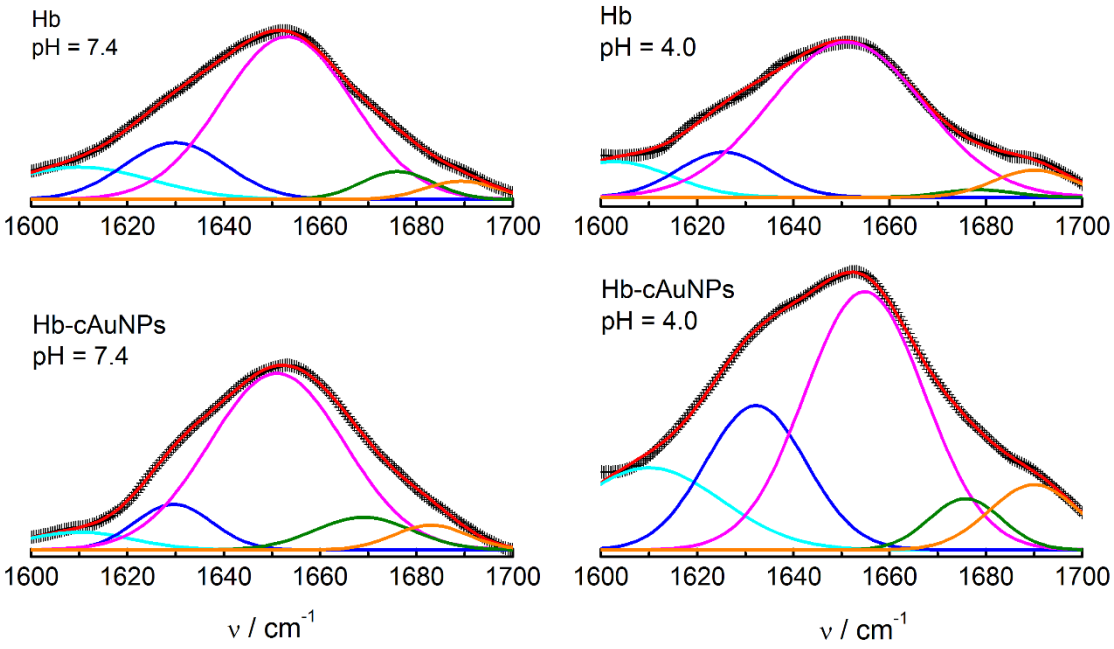

Figure 5. Deconvoluted ATR-IR spectra of Hb and Hb-cAuNPs at pH 7.4 and pH 4.0. (Hb) = 1.5 µM; (cAuNP) = 5 nM.

Native Hb molecules show IR bands at 1651 and 1545 cm^{-1} for amide I and amide II bands, respectively (Figure SI-3), with an intensity ratio amide I/II of 1.2. Because amides I and II vibration modes are approximately perpendicular to each other, the ratio of these two band intensities gives a way to qualitatively assess the conformation/orientation changes of the protein [33, 41, 42]. Upon bioconjugate formation, the amide I band does not change appreciably but the amide II shows an increase in intensity giving intensity ratios of 1.1, 1.05 and 1.05 for the bioconjugates formed by MUA-, c- and MP-AuNPs, respectively. The similarities within the bioconjugates and with the free protein are indicative that the Hb conformation do not change upon binding to the AuNPs.

For IR spectroscopy analysis, the bioconjugates have been formed by using a protein/nanoparticle molar ratio of 300/1. Under these conditions, most of the Hb monitored should be bound to the AuNPs and the interference of free protein is avoided. We have analyzed the amide I band by a non-linear fitting process by using Gaussian curves. The parameters have been selected by self-deconvolution and second derivative analyses. In all the cases studied the chosen parameters agree with literature reports: 1651-1658 cm^{-1}, α-helix, 1618-1642 cm^{-1}, β-sheet, 1666-1688 cm^{-1}, turns, 1618-1623 cm^{-1} (T), intermolecular aggregates

(A_1), 1683-1689 cm^{-1}, intramolecular aggregates (A_2) [32]. The increase in the A_1 motif can be facilitated in a crowded environment. In fact, as the hydrogen bonds can be formed between C=O and N-H groups of any polypeptide strands with which they come into contact, the consequence is that, when the proteins come together upon binding to the nanoparticle surface and form the protein *corona*, more hydrogen bonds between polypeptide chains in neighboring protein molecules can be formed without provoking protein unfolding [43].

Figure 5 shows the deconvoluted spectra corresponding to the free Hb and the Hb-AuNPs in 10 mM phosphate buffer at pH 7.4 and 4.0. There are minor differences in the parameters obtained in the fitting procedure (Table 1). In fact, the bioconjugates are very stable in solution at pH 7.4 (Figure 2, 3) and, no big changes in the protein structure are expected. However, if the bioconjugates are formed at pH 4.0, the system experiments some mildly aggregation. As it can be seen, the amide I signal for the bioconjugates at pH 4.0 is around 2.5-fold enhanced in respect to the signal corresponding to the free protein at the same concentration. This enhancement is due to a SEIRAS effect produced both for the interaction of the protein with the AuNP in the bioconjugate and for the presence of aggregates that form a nano-structured system near the Germanium crystal surface. The second fact that is absent at pH 7 should be the reason of the absence of SEIRAS effect under these conditions.

Table 1. Parameters obtained in the deconvolution of IR spectra of the Hb and Hb-cAuNPs bioconjugates at pH 7.4 and 4.0, shown in Figure 5.

	Wavenumber Position				**fwhm**				**% Area**			
	pH 7.4		pH 4.0		pH 7.4		pH 4.0		pH 7.4		pH 4.0	
Conformer	Hb	Hb-cAuNPs	Hb	Hb-cAuNPs	Hb	Hb-cAuNPs	Hb	Hb-cAuNPs	Hb	Hb-cAuNPs	Hb	Hb-cAuNPs
A1	1610	1610	1606	1610	30	22	23	30	8.3	5.5	11.4	17.7
β	1630	1629	1625	1630	21	16	19	21	10.4	10.3	11.9	21.8
α	1653	1651	1651	1655	27	28	32	25	66.8	70	68.8	46.2
T	1676	1659	1678	1675	15	20	15	15	10.7	9.1	1.6	5.6
A2	1689	1683	1690	1690	15	15	17	18	3.8	5.1	6.3	8.7

Apart of this enhancement effect, a small change in the shape of the amide I band can be observed. In fact, the deconvolution analysis (Table 1) indicates that the proteins forming the bioconjugates at pH 4, loose some of the α-helix structure while small increases in the β-sheet content together with the A_1 component are observed. The later effect can be the result of the stronger inter-protein interactions

probably through hydrogen bonds between the exposed chains of the individual Hb molecules in the aggregate state. It is interesting to note that the α-helix content does not significantly change in contrast with the important transformation from α-helix to β-sheet observed in the case of the bioconjugate Hb-silver NP [43].

4. Conclusions

The concept of protein corona has evolved in the last years as a new paradigm in the use of nanomaterials in biological systems and, in particular, in nanomedicine [3, 4, 13, 15, 44-47]. Many papers have dealt with the characterization of the formed bioconjugates addressing it under some specific experimental conditions [25, 36, 43]. However, one of the most important aspects in the behavior of these bioconjugates is the possible changes in the protein conformation upon interaction with the nanomaterials and how these changes affect their stability in a wide range of aqueous environments. In this sense, we have analyzed the experimental conditions where the bioconjugates of AuNPs stabilized by different capping agents (c-, MP- and MUA-) [30, 31, 48] and the protein Hb are stable in solution or form aggregates. Although the three surface-protected AuNPs show different stability profile depending on the chemical nature of the protecting molecules [37], the bioconjugates are very alike. The aggregation of the bioconjugates starts at the isoelectric point of the protein, independently of the capping ligand of the AuNPs. UV-visible spectroscopy, dynamic light scattering and zeta-potential measurements agree with this observation. This is a further evidence of the protein *corona* formation and an indication of the chemical identity change of the AuNP in the presence of proteins [3].

The protein conformation does not change upon interaction with the nanoparticle in the pH range where the bioconjugate remains stable in solution. However, a small change in secondary structure, as seen by ATR-IR spectroscopy, is observed when the bioconjugates form aggregates at lower pH.

The systematic characterization of AuNPs bioconjugates formed with a model protein as Hb can help in understanding the role of the protein *corona* in biological fluids and suggests that, when the chemical functionality of the nanoparticle surface is appropriate, the conformation of the proteins do not necessarily change upon adsorption.

Acknowledgements.

We thank the Ministerio de Economía y Competitividad (MINECO) (Projects CTQ2014-60227-R and CTQ-2015-71955-REDT Network of excellence Sensors and Biosensors), Junta de Andalucía (P10-FQM-6408) and University of Córdoba for financial support of this work.

References

[1] K. Cai, A.Z. Wang, L. Yin, J. Cheng, Bio-nano interface: The impact of biological environment on nanomaterials and their delivery properties, Journal of Controlled Release. http://dx.doi.org/10.1016/j.jconrel.2016.11.034 .

[2] A.E. Nel, L. Maedler, D. Velegol, T. Xia, E.M.V. Hoek, P. Somasundaran, F. Klaessig, V. Castranova, M. Thompson, Understanding biophysicochemical interactions at the nano-bio interface, Nat. Mater,, 8 (2009) 543-557.

[3] D. Walczyk, F.B. Bombelli, M.P. Monopoli, I. Lynch, K.A. Dawson, What the Cell "Sees" in Bionanoscience, J. Am. Chem. Soc., 132 (2010) 5761-5768.

[4] T. Cedervall, I. Lynch, S. Lindman, T. Berggard, E. Thulin, H. Nilsson, K.A. Dawson, S. Linse, Understanding the nanoparticle-protein corona using methods to quantify exchange rates and affinities of proteins for nanoparticles, Proc. Natl. Acad. Sci. U. S. A., 104 (2007) 2050-2055.

[5] T. Cedervall, I. Lynch, M. Foy, T. Berggad, S.C. Donnelly, G. Cagney, S. Linse, K.A. Dawson, Detailed identification of plasma proteins adsorbed on copolymer nanoparticles, Angew. Chem.-Int. Edit., 46 (2007) 5754-5756.

[6] M. Lundqvist, J. Stigler, G. Elia, I. Lynch, T. Cedervall, K.A. Dawson, Nanoparticle size and surface properties determine the protein corona with possible implications for biological impacts, Proc. Natl. Acad. Sci. U. S. A., 105 (2008) 14265-14270.

[7] M.P. Monopoli, F.B. Bombelli, K.A. Dawson, Nanobiotechnology. Nanoparticle coronas take shape, Nat. Nanotechnol., 6 (2011) 11-12.

[8] S.T. Yang, Y. Liu, Y.W. Wang, A.N. Cao, Biosafety and Bioapplication of Nanomaterials by Designing ProteinNanoparticle Interactions, Small, 9 (2013) 1635-1653.

[9] D. Docter, D. Westmeier, M. Markiewicz, S. Stolte, S.K. Knauer, R.H. Stauber, The nanoparticle biomolecule corona: lessons learned - challenge accepted?, Chem. Soc. Rev., 44 (2015) 6094-6121.

[10] P.M. Kelly, C. Aberg, E. Polo, A. O'Connell, J. Cookman, J. Fallon, Z. Krpetic, K.A. Dawson, Mapping protein binding sites on the biomolecular corona of nanoparticles, Nat. Nanotechnol., 10 (2015) 472-479.

[11] D.F. Moyano, V.M. Rotello, Nano Meets Biology: Structure and Function at the Nanoparticle Interface, Langmuir, 27 (2011) 10376-10385.

[12] S.R. Saptarshi, A. Duschl, A.L. Lopata, Interaction of nanoparticles with proteins: relation to bio-reactivity of the nanoparticle, J. Nanobiotechnol., 11 (2013).

[13] G. Caracciolo, O.C. Farokhzad, M. Mahmoudi, Biological Identity of Nanoparticles In Vivo: Clinical Implications of the Protein Corona, Trends Biotechnol., 35 (2017) 257-264.

[14] C.D. Walkey, J.B. Olsen, F. Song, R. Liu, H. Guo, D.W.H. Olsen, Y. Cohen, A. Emili, W.C.W. Chan, Protein Corona Fingerprinting Predicts the Cellular Interaction of Gold and Silver Nanoparticles, Acs Nano, 8 (2014) 2439-2455.
[15] K. Hamad-Schifferli, How can we exploit the protein corona?, Nanomedicine, 8 (2013) 1-3.
[16] K. Hamad-Schifferli, Exploiting the novel properties of protein coronas: emerging applications in nanomedicine, Nanomedicine, 10 (2015) 1663-1674.
[17] E. Casals, V.F. Puntes, Inorganic nanoparticle biomolecular corona: formation, evolution and biological impact, Nanomedicine, 7 (2012) 1917-1930.
[18] M. Mahmoudi, I. Lynch, M.R. Ejtehadi, M.P. Monopoli, F.B. Bombelli, S. Laurent, Protein-Nanoparticle Interactions: Opportunities and Challenges, Chem. Rev., 111 (2011) 5610-5637.
[19] M.P. Monopoli, C. Aberg, A. Salvati, K.A. Dawson, Biomolecular coronas provide the biological identity of nanosized materials, Nat. Nanotechnol., 7 (2012) 779-786.
[20] N. Goswami, K. Zheng, J. Xie, Bio-NCs - the marriage of ultrasmall metal nanoclusters with biomolecules, Nanoscale, 6 (2014) 13328-13347.
[21] Y.N. Zhao, X.X. Sun, G.N. Zhang, B.G. Trewyn, Slowing, II, V.S.Y. Lin, Interaction of Mesoporous Silica Nanoparticles with Human Red Blood Cell Membranes: Size and Surface Effects, Acs Nano, 5 (2011) 1366-1375.
[22] D. Drescher, T. Buechner, D. McNaughton, J. Kneipp, SERS reveals the specific interaction of silver and gold nanoparticles with hemoglobin and red blood cell components, Phys. Chem. Chem. Phys., 15 (2013) 5364-5373.
[23] R.T. Tom, A.K. Samal, T.S. Sreeprasad, T. Pradeep, Hemoprotein bioconjugates of gold and silver nanoparticles and gold nanorods: Structure-function correlations, Langmuir, 23 (2007) 1320-1325.
[24] D. Sahoo, P. Bhattacharya, H.K. Patra, P. Mandal, S. Chakravorti, Gold nanoparticle induced conformational changes in heme protein, J. Nanopart. Res., 13 (2011) 6755-6760.
[25] Q. Shao, P. Wu, P.A. Gu, X.Q. Xu, H. Zhang, C.X. Cai, Electrochemical and Spectroscopic Studies on the Conformational Structure of Hemoglobin Assembled on Gold Nanoparticles, J. Phys. Chem. B, 115 (2011) 8627-8637.
[26] S. Garabagiu, A spectroscopic study on the interaction between gold nanoparticles and hemoglobin, Mater. Res. Bull., 46 (2011) 2474-2477.
[27] W. Yang, L. Sun, J. Weng, L. Chen, Q. Zhang, Probing the interaction of bovine haemoglobin with gold nanoparticles, IET Nanobiotechnol, 6 (2012) 26-32.
[28] S. Garabagiu, Gold nanorods-hemoglobin bio-conjugate: Spectroscopy studies, J. Molec. Struct., 1031 (2013) 216-220.

[29] C.D. Keating, M.D. Musick, M.H. Keefe, M.J. Natan, Kinetics and thermodynamics of Au colloid monolayer self-assembly - Undergraduate experiments in surface and nanomaterials chemistry, J. Chem. Educ., 76 (1999) 949-955.
[30] A.J. Viudez, R. Madueno, T. Pineda, M. Blazquez, Stabilization of gold nanoparticles by 6-mercaptopurine monolayers. Effects of the solvent properties, J. Phys. Chem. B, 110 (2006) 17840-17847.
[31] E. Reyes, R. Madueno, M. Blazquez, T. Pineda, Facile Exchange of Ligands on the 6-Mercaptopurine-Monolayer Protected Gold Clusters Surface, J. Phys. Chem. C, 114 (2010) 15955-15962.
[32] H.H.M. M. Jackson, Protein Ligand Interactions: Structure and Spectroscopy, Oxford University Press, New York, 2001.
[33] M. Jackson, H.H. Mantsch, The Use and Misuse of FTIR Spectroscopy in the Determination of Protein-Structure, Crit. Rev. Biochem. Mol., 30 (1995) 95-120.
[34] W.K. Surewicz, H.H. Mantsch, New Insight into Protein Secondary Structure from Resolution-Enhanced Infrared-Spectra, Biochim. Biophys. Acta, 952 (1988) 115-130.
[35] A.C. Templeton, J.J. Pietron, R.W. Murray, P. Mulvaney, Solvent refractive index and core charge influences on the surface plasmon absorbance of alkanethiolate monolayer-protected gold clusters, J. Phys. Chem. B, 104 (2000) 564-570.
[36] F. Canaveras, R. Madueno, J.M. Sevilla, M. Blazquez, T. Pineda, Role of the Functionalization of the Gold Nanoparticle Surface on the Formation of Bioconjugates with Human Serum Albumin, J. Phys. Chem. C, 116 (2012) 10430-10437.
[37] B. Cárdenas, G. Sánchez-Obrero, R. Madueño, J.M. Sevilla, M. Blázquez, T. Pineda, Influence of the Global Charge of the Protein on the Stability of Lysozyme–AuNP Bioconjugates, J. Phys. Chem. C, 118 (2014) 22274-22283.
[38] M. Brunori, G. Amiconi, E. Antonini, J. Wyman, R. Zito, R. Fanelli, Transition between Acid and Alkaline Ferric Heme Proteins, Biochim. Biophys. Acta, 154 (1968) 315-322.
[39] J. Kunze, I. Burgess, R. Nichols, C. Buess-Herman, J. Lipkowski, Electrochemical evaluation of citrate adsorption on Au(111) and the stability of citrate-reduced gold colloids, J. Electroanal. Chem., 599 (2007) 147-159.
[40] D.M. Byler, H. Susi, Examination of the Secondary Structure of Protein by Deconvolved FTIR Spectra, Biopolymers, 25 (1986) 469-487.
[41] H. Fabian, L.P. Choo, G.I. Szendrei, M. Jackson, W.C. Halliday, L. Otvos, H.H. Mantsch, Infrared Spectroscopic Characterization of Alzheimer Plaques, Appl. Spectrosc., 47 (1993) 1513-1518.

[42] P. Roach, D. Farrar, C.C. Perry, Surface tailoring for controlled protein adsorption: Effect of topography at the nanometer scale and chemistry, J. Am. Chem. Soc., 128 (2006) 3939-3945.
[43] M. Mahato, P. Pal, T. Kamilya, R. Sarkar, A. Chaudhuri, G.B. Talapatra, Hemoglobin-Silver Interaction and Bioconjugate Formation: A Spectroscopic Study, J. Phys. Chem. B, 114 (2010) 7062-7070.
[44] I. Lynch, T. Cedervall, M. Lundqvist, C. Cabaleiro-Lago, S. Linse, K.A. Dawson, The nanoparticle - protein complex as a biological entity; a complex fluids and surface science challenge for the 21st century, Adv. Colloid Interface Sci., 134-35 (2007) 167-174.
[45] E. Casals, T. Pfaller, A. Duschl, G.J. Oostingh, V. Puntes, Time Evolution of the Nanoparticle Protein Corona, Acs Nano, 4 (2010) 3623-3632.
[46] V. Mirshafiee, R. Kim, S. Park, M. Mahmoudi, M.L. Kraft, Impact of protein pre-coating on the protein corona composition and nanoparticle cellular uptake, Biomaterials, 75 (2016) 295-304.
[47] F. Bertoli, D. Garry, M.P. Monopoli, A. Salvati, K.A. Dawson, The Intracellular Destiny of the Protein Corona: A Study on its Cellular Internalization and Evolution, Acs Nano, 10 (2016) 10471-10479.
[48] A.J. Viudez, R. Madueno, M. Blazquez, T. Pineda, Synthesis, Characterization, and Double Layer Capacitance Charging of Nanoclusters Protected by 6-Mercaptopurine, J. Phys. Chem. C, 113 (2009) 5186-5192.

Graphical Abstract.